



Diagenetic history and porosity evolution of Upper Carboniferous sandstones from the Spring Valley #1 well, Maritimes Basin, Canada—implications for reservoir development

G. Chi^{a,*}, P.S. Giles^b, M.A. Williamson^b, D. Lavoie^a, R. Bertrand^c

^a Geological Survey of Canada—Quebec Division, 880 Chemin Ste-Foy, P.O. Box 7500, Ste-Foy, Quebec, Canada G1V 4C7

^b Geological Survey of Canada—Atlantic Division, P.O. Box 1006, Dartmouth, Nova Scotia, Canada B2Y 4A2

^c INRS-Eau, Terre et Environnement, 880 Chemin Ste-Foy, P.O. Box 7500, Ste-Foy, Quebec, Canada G1V 4C7

Received 15 March 2001; received in revised form 30 June 2002; accepted 30 September 2002

Abstract

Eighty-two core samples were collected from the Spring Valley #1 well which penetrates the Upper Carboniferous strata in the Late Devonian–Early Permian Maritimes Basin. The strata consist of alternating sandstones and mudstones deposited in a continental environment. The objective of this study is to characterize the relationship of sandstone porosity with depth, and to investigate the diagenetic processes related to the porosity evolution. Porosity values estimated from point counting range from 0% to 27.8%, but are mostly between 5% and 20%. Except samples that are significantly cemented by calcite, porosity values clearly decrease with depth. Two phases of calcite cement were distinguished based on Cathodoluminescence, with the early phase being largely dissolved and preserved as minor relicts in the later phase. Feldspar dissolution was extensive and contributed significantly to the development of secondary porosity. Quartz cementation was widespread and increased with depth. Fluid inclusions recorded in calcite and quartz cements indicate that interstitial fluids in the upper part of the stratigraphic column were dominated by waters with salinity lower than that of seawater, the middle part was first dominated by low-salinity waters, then invaded by brines, and the lower part was dominated by brines. Homogenization temperatures of fluid inclusions generally increase with depth and suggest a paleogeothermal gradient of 25 °C/km, which is broadly consistent with that indicated by vitrinite reflectance data. An erosion of 1.1–2.4 (mean 1.75) km of strata is inferred to have taken place above the stratigraphic column. $\delta^{18}\text{O}$ values of calcite cements (mainly from the late phase) decrease with depth, implying increasing temperatures of formation, as also suggested by fluid-inclusion data. $\delta^{13}\text{C}$ values of calcite cements range from -13.4‰ to -5.7‰ , suggesting that organic matter was an important carbon source for calcite cements. A comparison of the porosity data with a theoretical compaction curve indicates that the upper and middle parts of the stratigraphic column show higher-than-normal porosity values, which are related to significant calcite and feldspar dissolution. Meteoric incursion and carboxylic acids generated from organic maturation were probably responsible for the abundant dissolution events.

© 2003 Elsevier B.V. All rights reserved.

Keywords: Maritimes Basin; Spring Valley #1 well; Sandstone porosity; Diagenesis; Hydrocarbons; Fluid inclusions; Stable isotopes

* Corresponding author. Present address: Department of Geology, University of Regina, Saskatchewan, Canada S4S 0A2. Tel.: +1-306-585-4583; fax: +1-306-585-5433.

E-mail address: guoxiang.chi@uregina.ca (G. Chi).

1. Introduction

The Maritimes Basin is a late Paleozoic intracontinental successor basin developed upon early Paleozoic and older basements in the Northern Appalachians (Williams, 1974; van de Poll et al., 1995). It underlies a significant part of the Gulf of St. Lawrence, New Brunswick, Nova Scotia, the entire Prince Edward Island, and a small part of Newfoundland and Quebec (Fig. 1A). It contains important coal, evaporites, oil, gas, oil shales, and base metal resources (van de Poll et al., 1995).

The hydrocarbon potential of the Maritimes Basin has been demonstrated by the occurrence of one small oil and gas field (Stony Creek, New Brunswick), a number of oil seeps and shows, oil shales, and coal-derived methane (Williams, 1974; Kalkreuth and Macauley, 1987; Chowdhury et al., 1991; Fowler et al., 1993; Hamblin et al., 1995; Chi and Savard, 1999). Although more than 300 petroleum wells have been drilled in the Maritimes Basin (mainly in the Stony Creek field), only 11 have been drilled in the offshore areas. Since these offshore areas comprise more than 70% of the total basin surface (Fig. 1A), it follows that the basin is largely

under-explored (Bibby and Shimeld, 2000). Of the key elements of petroleum systems in the Maritimes Basin, reservoir quality is the most poorly understood (Bibby and Shimeld, 2000). Few diagenetic studies have been carried out to decipher the porosity history and the factors controlling the reservoir quality in the sandstones (Chowdhury and Noble, 1992; Gibling and Nguyen, 1999). The present study documents detailed petrographic, fluid-inclusion, and stable isotope data of sandstones from the Spring Valley #1 well in Prince Edward Island. This well penetrates the upper part of the basin stratigraphy, and is the only one that has cored the entire Upper Carboniferous succession. The objective of this study is to characterize the porosity-depth patterns and their controlling factors, thus providing a reference for understanding the diagenetic history and porosity evolution of equivalent sandstones in other parts of the basin.

2. Geological setting

The Maritimes Basin is filled with Late Devonian to Early Permian continental and marine sediments

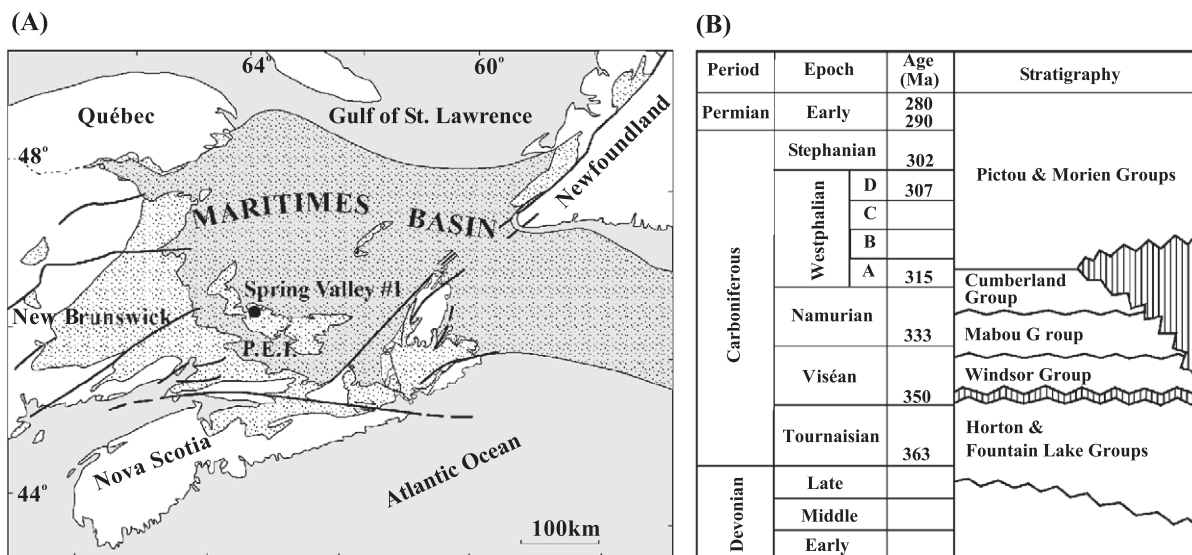


Fig. 1. (A) The regional extension of the Maritimes Basin, and the location of the Spring Valley #1 well on Prince Edward Island. (B) General stratigraphic column of the Maritimes Basin (modified from Ryan et al., 1991; St. Peter, 1993). Vertical lines represent depositional hiatuses and/or rocks removed by erosion.

(Ryan et al., 1991; St. Peter, 1993) (Fig. 1B). Following the middle Devonian Acadian Orogeny, and until the latest Tournaisian, continental clastic rocks were deposited in fault-bounded basins and subsequently in laterally extensive sag basins. These deposits are assigned regionally to the Horton and Fountain Lake groups. In the Viséan, a succession of marine to continental sediments was deposited, forming the Windsor Group. At the base of this marine succession, a decameter-thick layer of limestone unconformably overlies the Horton Group rocks (Lavoie and Sami, 1998). This carbonate unit (the Macumber Formation) is succeeded by a thick succession of evaporites with intercalated carbonates developed in a shallow, fluctuating, marine environment. With the gradual withdrawal of the Windsor Sea, a mixed succession of clastic and carbonate sediments, with increasing continental components, was deposited, forming the upper part of the Windsor Group. Above the Windsor Group, sedimentation in the Maritimes Basin occurred predominantly in continental environments, forming the Mabou, Cumberland, Morien and Pictou groups. The strata of the Maritimes Basin have been affected by several tectonic events, as indicated by major unconformities between the Horton and Windsor, Mabou and Cumberland, and between Cumberland and Pictou groups (Fig. 1B; St. Peter, 1993). The strata of the Pictou Group are generally flat-lying to gently-dipping, whereas older strata are folded and faulted to variable degrees, especially near the basin margin.

The Spring Valley #1 well is located in west-central Prince Edward Island (Fig. 1A). It penetrated the Naufrage, Cable Head, Green Gables, and Bradelle formations and was completed in the Shepody Formation at a depth of 1706 m (Giles and Utting, 1999) (Fig. 2). The strata from the Bradelle to Naufrage formations range in age from Westphalian C to Stephanian, and are assigned to the Pictou Group. The Shepody Formation probably belongs to the late Viséan to possibly earliest Namurian, and is assigned to the Mabou Group. Strata equivalent to the Cumberland Group in its type area are not represented in the Spring Valley #1 well. Biostratigraphic data suggest a significant unconformity between the Shepody and Bradelle formations.

All strata cored in the Spring Valley #1 well are typified by alternating sandstones (locally conglomerates)

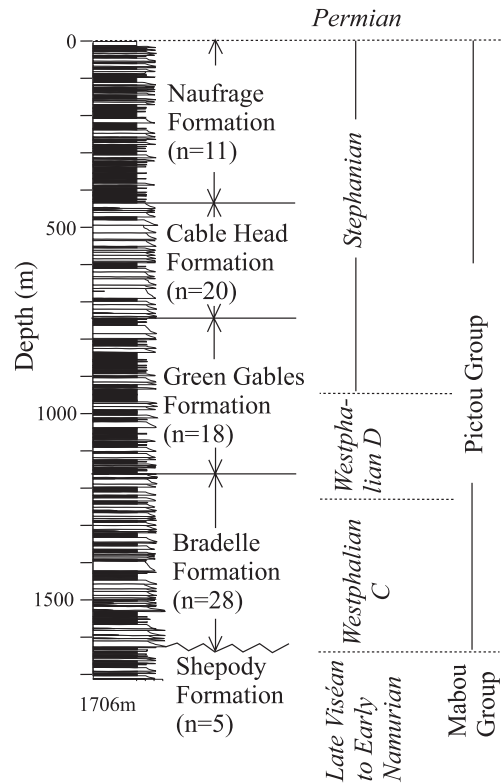


Fig. 2. Stratigraphic column of the Spring Valley #1 well (after Giles and Utting, 1999), also showing the number of core samples in each formation.

erates) and mudstones or shales, with sandstones being more abundant in the Cable Head and Bradelle formations, and mudstones/shales dominating the Naufrage, Green Gables, and Shepody formations (Fig. 2).

3. Methods of study

The samples were impregnated with blue-dyed epoxy for petrographic examination. Estimation of the percentages of cements, detrital grains, and porosity was made on thin sections with a Swift counter ($n = 300$). Artifact porosity introduced in sample preparation (Pittman, 1992) is probably small because oversized pores are uncommon. Diagenetic features and cross-cutting relationships were examined using conventional thin-section petrography and cathodoluminescence (CL). The CL was run with a Premier

Table 1
Depth, porosity, and components of the sandstone samples from the Spring Valley #1 well

Sample no.	Formation	Lithology	Depth (m)	Porosity ^a	Detrital quartz	Detrital feldspar	Lithic grains	Quartz overgrowth	Feldspar overgrowth	Carbonate cement
GC99-1	Naufrage	Red mudstone	111.60							
GC99-2		Red sandstone	107.30	0.6	18.2	1.8	40.0	0.2	0.2	39.0
GC99-3		Red sandstone	78.41	20.8	36.0	6.6	36.2	0.4	0.0	0.0
GC99-4		Red sandstone	42.30	20.0	39.4	12.8	24.8	0.4	0.4	2.2
GC99-5		Red mudstone	14.61							
GC99-6		Red sandstone	136.30	19.6	34.4	16.4	28.2	0.8	0.0	0.6
GC99-7		Red sandstone	155.01	19.6	33.8	9.6	36.8	0.2	0.2	0.0
GC99-8		Red sandstone	212.76	18.6	37.4	8.4	26.8	0.2	0.4	8.2
GC99-9		Red sandstone	242.03	2.4	30.2	7.8	41.2	0.2	0.0	18.2
GC99-10		Red sandstone	302.50	27.8	32.8	11.2	24.8	1.6	0.4	1.4
GC99-11		Red sandstone	379.59	25.2	37.4	8.6	25.2	1.8	0.0	1.8
GC99-12		Red sandstone	432.30	22.2	36.0	10.8	27.0	1.2	0.2	2.6
GC99-13		Red sandstone	464.64	19.0	30.6	18.8	29.6	0.6	0.0	1.4
GC99-14		Red sandstone	482.00	14.6	35.8	14.0	31.6	2.2	0.0	1.8
GC99-15		Red sandstone	495.58	1.9	26.0	12.0	26.5	0.3	0.0	33.3
GC99-16	Cable Head	Red sandstone	490.04	17.4	32.4	17.4	31.0	0.8	0.0	1.0
GC99-17		Red sandstone	517.80	19.6	30.6	16.6	30.8	1.0	0.0	1.4
GC99-18		Red sandstone	534.93	19.2	34.2	17.7	27.7	1.2	0.0	0.0
GC99-19		Red sandstone	572.00	20.0	35.7	15.5	25.9	1.7	0.2	1.0
GC99-20		Red sandstone	584.15	0.0	27.6	8.0	31.1	0.0	0.0	33.3
GC99-21		Red sandstone	576.67	0.0	12.0	9.6	60.4	0.0	0.0	18.0
GC99-22		Grey sandstone	590.80	19.6	37.4	15.0	25.4	0.4	0.0	2.2
GC99-23		Red mudstone	596.67							
GC99-24		Red sandstone	608.01	15.4	38.8	12.6	32.4	0.2	0.2	0.4
GC99-25		Red sandstone	626.36	25.6	32.4	19.4	20.4	0.0	0.0	2.2
GC99-26	Red sandstone	642.19	15.4	41.2	22.6	20.2	0.4	0.0	0.2	
GC99-27	Red sandstone	669.69	15.8	39.4	18.2	25.8	0.8	0.0	0.0	
GC99-28	Red sandstone	693.42	0.0	21.6	9.3	37.8	0.3	0.0	31.0	
GC99-29	Red sandstone	721.03	15.0	36.0	21.4	24.4	1.8	0.0	1.4	
GC99-30	Red sandstone	726.97	14.2	32.4	25.8	23.0	1.4	0.0	3.2	
GC99-31	Red sandstone	736.03	14.6	34.4	32.4	12.6	1.6	0.0	4.4	
GC99-32	Green Gables	Red sandstone	765.37	13.8	39.4	21.6	19.2	3.4	0.0	2.6
GC99-33		Grey sandstone	775.37	22.2	34.0	20.0	22.6	1.0	0.0	0.2
GC99-34		Grey sandstone	792.47	17.0	39.0	16.8	24.4	2.0	0.0	0.8
GC99-35		Red sandstone	815.33	19.6	30.2	8.8	40.2	0.6	0.0	0.6
GC99-36		Red sandstone	824.57	13.4	39.4	9.4	37.4	0.4	0.0	0.0
GC99-37		Red mudstone	849.41							
GC99-38		Red sandstone	888.62	9.4	47.0	3.2	39.0	0.6	0.0	0.8
GC99-39		Red sandstone	903.80	9.8	38.8	7.4	42.4	0.8	0.2	0.6
GC99-40		Grey sandstone	912.75	15.6	26.4	11.2	43.6	1.2	0.0	2.0
GC99-41		Grey sandstone	925.40	9.8	34.8	9.2	42.4	2.6	0.0	1.2
GC99-42	Grey mudstone	966.84								
GC99-43	Grey sandstone	980.12	16.0	39.6	11.2	32.2	0.4	0.0	0.6	
GC99-44	Red sandstone	998.51	0.0	18.3	6.3	39.8	0.0	0.0	35.6	
GC99-45	Grey sandstone	1025.77	14.0	53.8	2.4	28.6	0.2	0.0	1.0	
GC99-46	Grey sandstone	1065.79	11.4	48.2	4.0	35.0	1.4	0.0	0.0	
GC99-47	Grey sandstone	1095.44	11.6	35.8	9.2	32.0	5.2	0.0	6.2	
GC99-48	Grey sandstone	1107.45	14.4	34.0	5.6	40.0	4.8	0.2	1.0	
GC99-49	Grey sandstone	1138.87	19.4	55.2	3.4	18.8	2.6	0.0	0.6	
GC99-50	Bradelle	Grey sandstone	1160.07	13.0	43.2	6.8	33.4	3.4	0.0	0.2
GC99-51		Grey sandstone	1175.22	14.0	40.2	5.0	36.2	4.0	0.0	0.6
GC99-52		Grey sandstone	1187.22	16.6	39.6	8.2	31.2	3.2	0.2	1.0

Table 1 (continued)

Sample no.	Formation	Lithology	Depth (m)	Porosity ^a	Detrital quartz	Detrital feldspar	Lithic grains	Quartz overgrowth	Feldspar overgrowth	Carbonate cement
GC99-53		Calcite replacing plants	1209.96							
GC99-54		Grey sandstone	1225.92	9.6	43.2	5.6	40.0	1.4	0.0	0.2
GC99-55		Grey sandstone	1247.22	4.6	46.0	6.6	39.8	3.0	0.0	0.0
GC99-56		Grey sandstone	1265.22	13.2	46.0	3.0	35.0	2.8	0.0	0.0
GC99-57		Grey sandstone	1276.02	7.0	38.4	11.0	40.0	3.4	0.2	0.0
GC99-58		Grey sandstone	1297.72	5.6	53.0	11.0	29.4	1.0	0.0	0.0
GC99-59		Grey mudstone	1325.91							
GC99-60		Grey sandstone	1334.92	3.6	46.8	10.4	36.8	2.4	0.0	0.0
GC99-61		Grey sandstone	2355.22	10.0	49.0	3.8	37.0	0.4	0.0	0.0
GC99-62		Grey sandstone	1380.82	8.4	42.4	6.8	39.6	2.8	0.0	0.0
GC99-63		Grey sandstone	1383.83	9.8	58.0	0.8	28.0	3.0	0.0	0.4
GC99-64		Grey sandstone	1394.82	6.6	39.9	8.6	43.6	1.3	0.0	0.0
GC99-65		Grey sandstone	1417.75	5.6	53.3	1.6	34.2	5.3	0.0	0.0
GC99-66		Red mudstone	1435.29							
GC99-67		Grey sandstone	1448.22	4.9	34.6	8.6	48.3	3.6	0.0	0.0
GC99-68		Grey sandstone	1455.35	3.6	41.3	5.3	44.5	5.3	0.0	0.0
GC99-69		Grey sandstone	1475.82	4.6	32.3	6.6	54.6	1.6	0.0	0.3
GC99-70		Grey sandstone	1482.95	5.6	38.3	7.3	44.8	4.0	0.0	0.0
GC99-71		Calcite replacing plants	1489.46							
GC99-72		Grey sandstone	1498.43	2.6	36.0	7.3	50.1	4.0	0.0	0.0
GC99-73		Grey sandstone	1518.56	3.0	34.3	5.6	52.8	4.3	0.0	0.0
GC99-74		Grey sandstone	1565.22	6.9	36.3	6.3	45.5	5.0	0.0	0.0
GC99-75		Grey sandstone	1586.42	3.6	41.0	5.6	41.8	7.0	0.0	1.0
GC99-76		Grey sandstone	1603.63	6.0	34.0	2.6	53.8	3.6	0.0	0.0
GC99-77		Grey sandstone	1619.72	5.6	32.6	13.6	41.6	5.6	0.0	1.0
GC99-78	Shepody	Grey sandstone	1652.22	0.3	35.6	7.6	35.2	1.0	0.0	20.3
GC99-79		Grey sandstone	1665.43	4.9	50.0	4.6	34.5	4.0	0.0	2.0
GC99-80		Red sandstone	1685.47	0.6	34.3	5.0	37.5	9.3	0.0	13.3
GC99-81		Red sandstone	1688.22	2.3	50.0	4.3	38.8	3.0	0.0	1.6
GC99-82		Red sandstone	1703.75	5.0	41.0	6.6	44.1	2.3	0.0	1.0

^a Some pores are partly filled with clay minerals.

American Technologies ELM-3 luminescope system at 13 KV and 0.6 MA. The staining method of Dickson (1965) was used to further characterize the carbonate phases.

Homogenization and ice-melting temperatures of fluid inclusions were measured with a U.S.G.S. Heating/Freezing stage, with the precision being better than ± 1 and ± 0.2 °C, respectively. After microthermometric runs, the fluid inclusion chips were checked with CL to identify the carbonate phases that host the fluid inclusions.

Carbon and oxygen isotope analyses were conducted in the Delta Lab in GSC-Quebec. CO₂ liberated from carbonates, sampled with a Jansen micro-sampler, was analyzed with a VG-SIRA 12 mass

spectrometer. The analytical precision is better than ± 0.1 ‰ for both $\delta^{13}\text{C}$ and $\delta^{18}\text{O}$.

Organic matter (OM) concentrates (kerogen) were obtained following the method described by Bertrand and Héroux (1987). Transparent strew mounts were prepared, and polished, according to the method of Bertrand et al. (1985). A Zeiss II photo-reflectometer microscope with transmitted and reflected light capability was used to measure reflectance at 546 nm wavelength with a 40× oil-immersion objective (1.515 refractive index oil). Spots selected for measurement were approximately 3 μm on the polished surface of the kerogen. Reflectance was measured on randomly oriented organic particles under non-polarized reflected light. Microscopic identification of

kerogen is based on morphology and optical properties, according to the methods described by the International Commission of Coal Petrology (Taylor et al., 1998).

4. Petrography

A total of 82 core samples were collected and prepared for thin sections (Fig. 2). Seventy-three of these are sandstones. The sandstones are either red or gray in hand specimen. Red-colored sandstones are dominant in the upper part of the stratigraphic column, from the middle of the Green Gables Formation to the top of the Naufrage Formation (Table 1). The sandstones are mostly medium- (0.25–0.5 mm) and fine-grained (0.125–0.25 mm), moderately sorted, poorly rounded, and composed of quartz, feldspar, and lithic grains. On a QFL diagram, most Naufrage and Cable Head samples plot in the feldspathic litharenite field, most Bradelle and Shepody samples in the litharenite field, whereas the Green Gables samples are equally distributed in the two fields (Fig. 3).

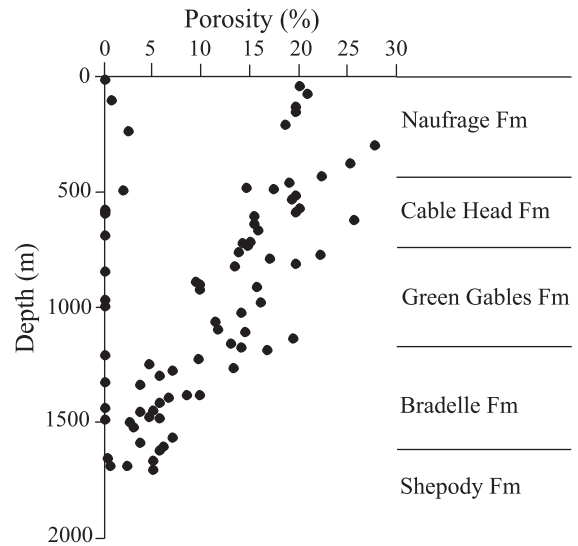


Fig. 4. Distribution of porosities with respect to drill depth of the Spring Valley #1 well.

The porosity values of the sandstones range from 0% to 27.8%, but are mostly between 5% and 20% (Table 1). Notwithstanding samples that are signifi-

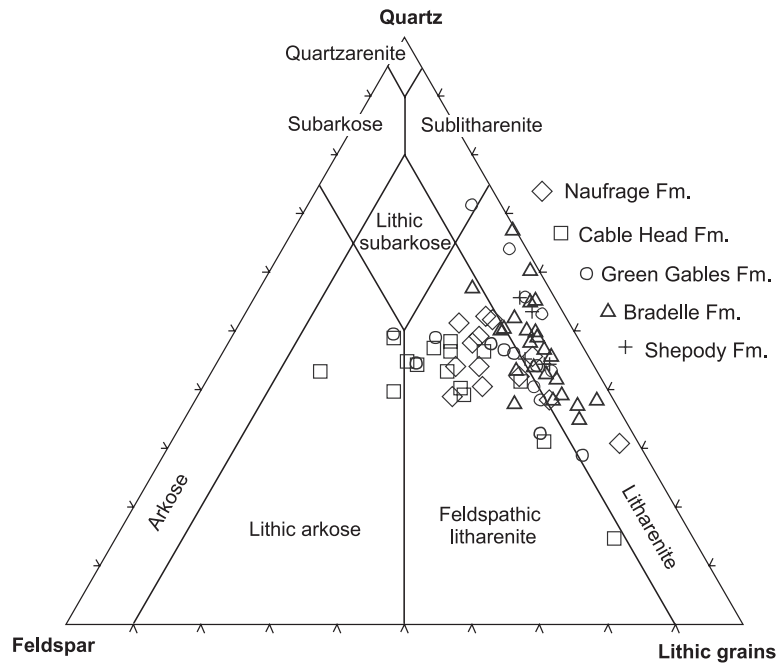


Fig. 3. Quartz-feldspar-lithic grain (QFL) diagram showing the composition of the detrital grains of the sandstones in the McBride's 1963 classification scheme (Blatt, 1992).

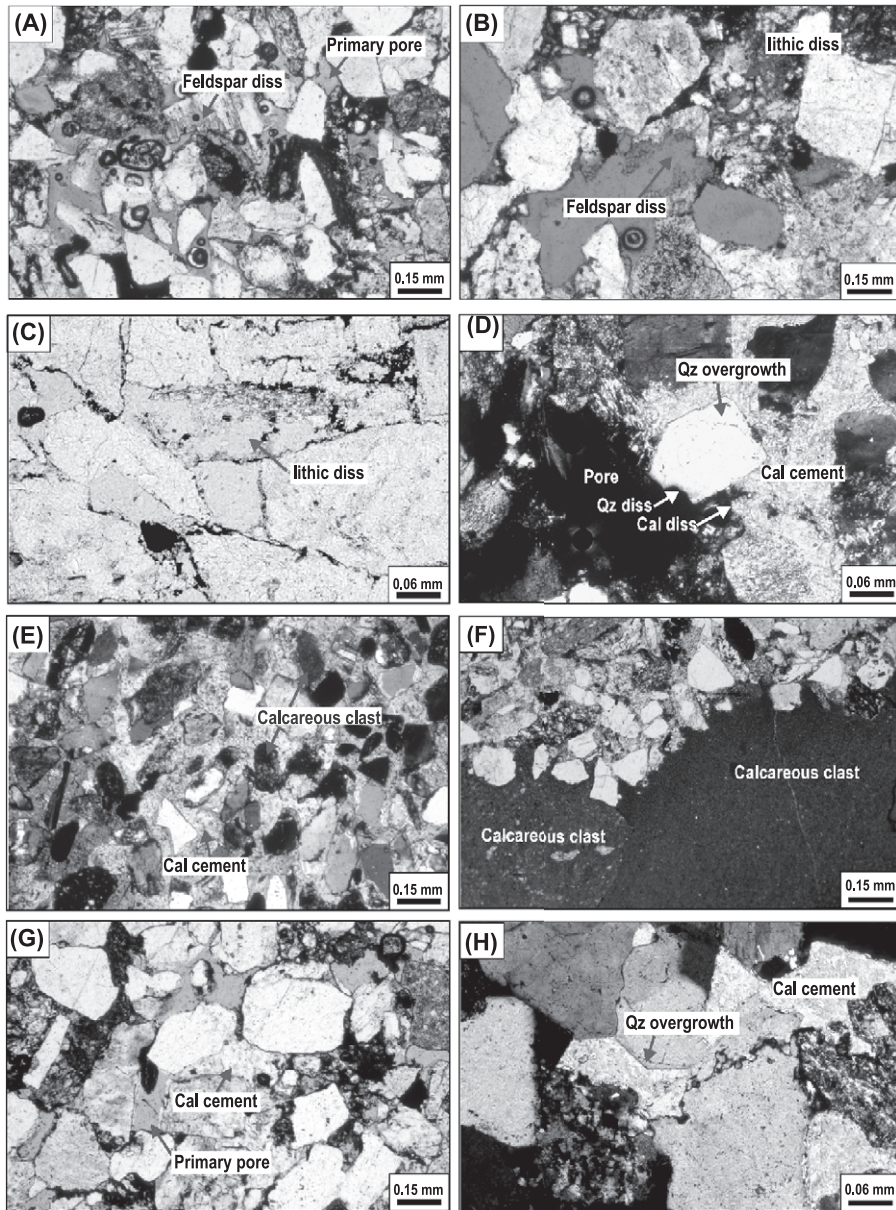


Fig. 5. Photomicrographs showing various petrographic features of sandstones from the Spring Valley #1 well. (A) Primary pores and secondary pores resulting from feldspar dissolution; GC99-3, plane light. (B) Dissolution of feldspars and lithic grains; GC99-18, plane light. (C) Dissolution of lithic grains; GC99-14, plane light. (D) Calcite cement postdating quartz cement and dissolution of calcite cement and quartz; GC99-25, crossed nicols. (E) Abundance of calcite cements and presence of calcareous clasts; GC99-2, crossed nicols. (F) Detrital grains “sinking” into the edge of calcareous clasts, indicating the soft nature of the calcareous clasts during compaction; GC99-21, plane light. (G) Calcite cement partly supporting the detrital grains; GC99-4, plane light. (H) Quartz overgrowth showing euhedral edge in contact with calcite cement; GC99-12, crossed nicols. (I) Two phases of calcite cements, with the first phase (dull) occurring as major components in the calcareous clast and as relicts in the second phase (orange); GC99-28, CL. (J) Two phases of calcite cements, with the first phase (dull to non-luminescent) occurring as relicts in the second phase (orange); GC99-2, CL. (K) Left: Interstitial calcite cement containing two phases (early non-luminescent phase occurring as relicts in a later phase of orange luminescence); right: calcite cement in a vein (second phase); GC99-2, CL. (L) Feldspar dissolution pores filled with phase-2 calcite cement, and not with phase-1 calcite cement; GC99-28, CL. (M) Two generations of quartz overgrowth; GC99-50, plane light. (N) Calcite cement postdated by green kaolinite; GC99-8, plane light.

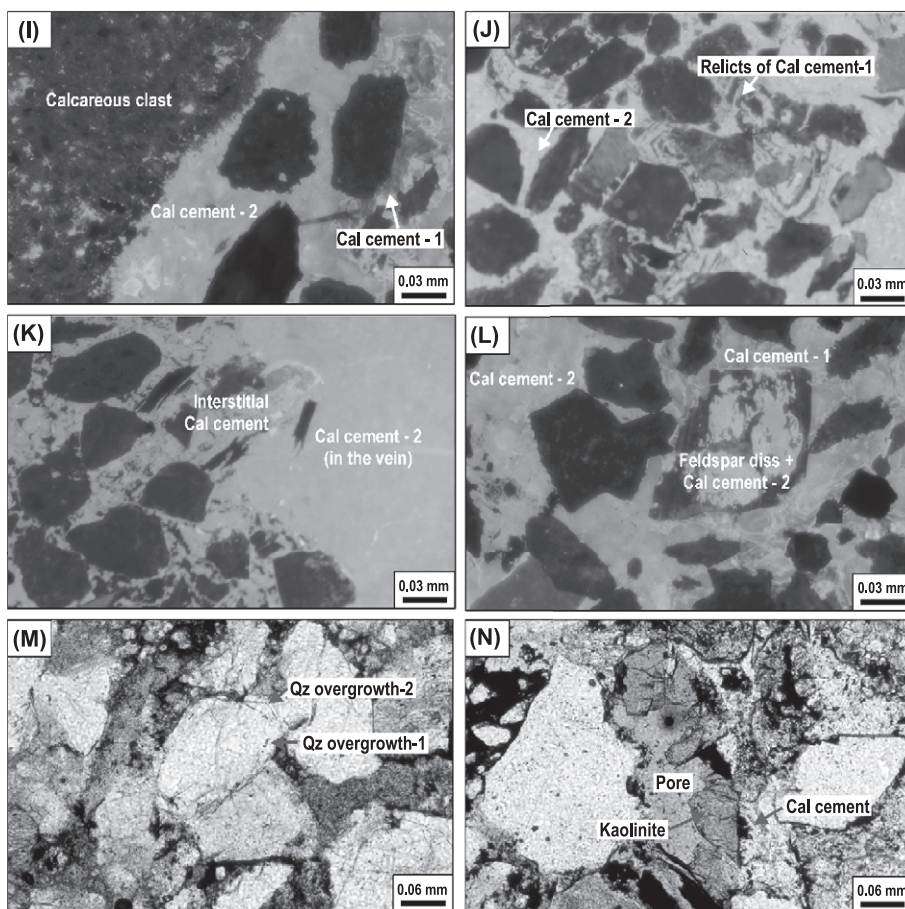


Fig. 5 (continued).

cantly cemented by calcite, porosity clearly decreases with depth (Fig. 4). The sizes of the pores range similarly to those of the detrital grains. Both primary and secondary porosities are present (Fig. 5A). Fractures are occasionally observed, and are typically filled with calcite (occasionally barite). Secondary porosity is mainly associated with the dissolution of feldspar (Fig. 5A and B), lithic grains (Fig. 5B and C), and calcite cement (Fig. 5D).

Calcite cements are ubiquitous in the sandstones, their proportions varying from near zero to as much as 39% (Table 1). In some samples, porosity is completely occluded by calcite cements, and detrital grains appear to float in calcite cements (Fig. 5E). These samples are characterized by the presence of calcareous clasts (Fig. 5E), some of which appear to

have been soft during compaction, as indicated by detrital quartz "sinking" into them (Fig. 5F). In most samples, however, calcite cements only partly fill porosity (Fig. 5G), leaving much open space, part of which could have resulted from later dissolution of the calcite cements. Calcite cements in the Naufrage Formation and the upper part of the Cable Head Formation are Fe-poor, whereas those in the underlying formations are mainly Fe-enriched, as indicated by staining. In two samples, calcite replaced fossil plants with well-preserved cells, indicating early replacement. Under CL, two phases of calcite cement are ubiquitous in all samples: phase 1 is non-luminescent or very dull, locally zoned, whereas phase 2 shows orange luminescence with or without relatively dull zones. Phase 2 is volumetrically much more important

Diagenetic events

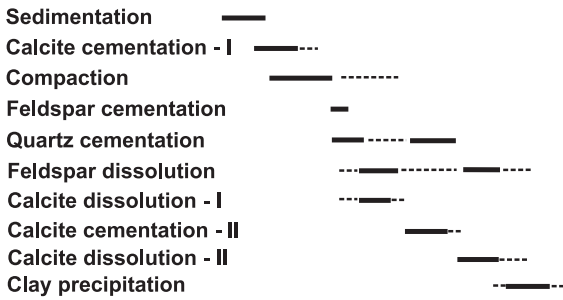


Fig. 6. General paragenetic succession recorded in sandstones of the Spring Valley #1 well.

than phase 1. Where sandstones are cut by veins, calcite in the veins is transitional to the phase 2 calcite in the matrix. Phase 1 calcite is the predominant calcite type in calcareous clasts, and it commonly occurs as relicts in phase 2 calcite (Fig. 5I, J, K and

L). The relicts of type-1 calcite are most abundant in sandstones with massive calcite cement. Secondary porosity associated with feldspar and lithic grain dissolution are commonly filled with phase 2 calcite, but not with phase 1 calcite (Fig. 5L), suggesting that phase 1 calcite was present before significant feldspar and lithic grain dissolution.

Quartz cements commonly occur as overgrowths on detrital quartz grains. Where calcite and quartz cements coexist, the edge of quartz cement may be irregular or rounded and overlain by calcite cement (Fig. 5D), indicating that calcite cements postdate quartz overgrowths. In many cases, however, the edge of quartz overgrowth is euhedral and appears to be in a growth compromise relationship with calcite cements (Fig. 5H). This may suggest that either the calcite and quartz were precipitated contemporaneously, or calcite postdated quartz precipitation. In a few cases, two phases of quartz overgrowth can be recognized, with a dust line between them (Fig. 5M).

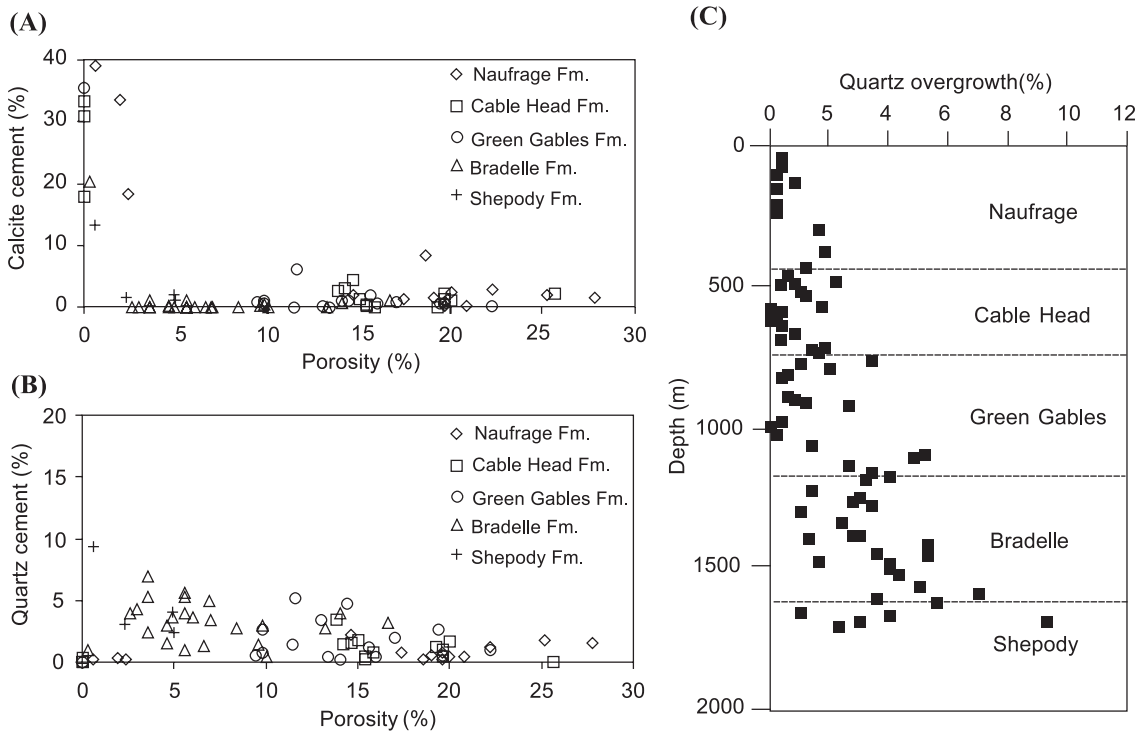


Fig. 7. (A) Correlation between abundance of calcite cements and porosity values. (B) Correlation between percentages of quartz cement and porosity values. (C) Variation of percentages of quartz cements with respect to drill depth.

Table 2
Fluid-inclusion microthermometric data

Sample no. (Formation)	Host mineral	Occurrence	Size (μm)	$T_{\text{m-ice}}(^{\circ}\text{C})$		Salinity (wt.% NaCl equiv.)		$T_{\text{h}}(^{\circ}\text{C})$		
				Range	Mean (n)	Range	Mean (n)	Range	Mean (n)	
GC99-2 (Naufrage)	Calcite cement-1	Random	9	–2.3	–2.3 (1)	3.9	3.9 (1)	all liquid	all liquid	
		Random	5–9	–1.1– –1.6	–1.4 (2)	1.9–2.7	2.3 (2)	all liquid	all liquid	
		Isolated	8	–1.1	–1.1 (1)	1.9	1.9 (1)	all liquid	all liquid	
	Calcite cement-2	Random	6–16	–	–	–	–	74.4–92.4	81.2 (4)	
		Random	4–9	–0.6– –1.0	–0.8 (2)	1.0–1.7	1.4 (2)	82.1–93.8	87.7 (4)	
		Isolated	10	–0.3	–0.3 (1)	0.5	0.5 (1)	66.9	66.9 (1)	
		Random	6–8	–0.6– –0.8	–0.2 (2)	1.0–1.4	1.2 (2)	73.3–79.0	75.9 (3)	
		Random	4–12	–0.2– –0.4	–0.3 (2)	0.4–0.7	0.6 (2)	72.9–77.5	75.2 (2)	
		Isolated	8	–	–	–	–	79.8	79.8 (1)	
		Cluster	6	–0.4	–0.4 (1)	0.7	0.7 (1)	67.7	67.7 (1)	
	Calcite cement-2 (vein)	Cluster	13–14	–0.6	–0.6 (1)	1.0	1.0 (1)	100.0–103.2	101.6 (2)	
		Cluster	9–12	–0.6	–0.6 (1)	1.0	1.0 (1)	82.8–91.2	87.0 (2)	
		Isolated	9	–1.0	–1.0 (1)	1.7	1.7 (1)	112.1	112.1 (1)	
GC99-9 (Naufrage)	Calcite cement-1	Isolated	9	–0.6	–0.6 (1)	1.0	1.0 (1)	all liquid	all liquid	
		Isolated	8	–	–	–	–	56.4	56.4 (1)	
	Calcite cement-2	Isolated	9	–0.4	–0.4 (1)	0.7	0.7 (1)	97.7	97.7 (1)	
		Isolated	7	–1.1	–1.1 (1)	1.9	1.9 (1)	101.8	101.8 (1)	
		Isolated	8	–	–	–	–	72.9	72.9 (1)	
GC99-11 (Naufrage)	Quartz cement	Isolated	11	–2.6	–2.6 (1)	4.3	4.3 (1)	104.4	104.4	
		Isolated	15	–	–	–	–	53.1	53.1 (1)	
	Calcite cement-1 cement-2	Isolated	7	–0.6	–0.6 (1)	1.0	1.0 (1)	all liquid	all liquid	
		Isolated	7	–0.6	–0.6 (1)	1.0	1.0 (1)	all liquid	all liquid	
		Isolated	10	–0.6	–0.6 (1)	1.0	1.0 (1)	all liquid	all liquid	
		Isolated	7	–0.3	–0.3 (1)	0.5	0.5 (1)	88.0	88.0 (1)	
		Scattered	6–12	–0.2– –0.4	–0.3 (3)	0.4–0.7	0.6 (2)	66.3–80.5	74.7 (4)	
		Isolated	10	–22.1	–22.1 (1)	23.4	23.4 (1)	88.0	88.0 (1)	
		Isolated	8	–22.1	–22.1 (1)	23.4	23.4 (1)	92.5	92.5 (1)	
		Isolated	7	–22.2	–22.2 (1)	23.4	23.4 (1)	79.3	79.3 (1)	
		Isolated	12	–22.4	–22.4	23.5	23.5 (1)	86.3	86.3 (1)	
Isolated	14	–21.0	–21.0 (1)	23.0	23.0 (1)	85.5	85.5 (1)			
GC00-15 (Naufrage)	Calcite cement-2	Isolated	5	–22.7	–22.7 (1)	23.5	23.5 (1)	75.5	75.5 (1)	
		Isolated	7	–2.2	–2.2 (1)	3.7	3.7 (1)	87.9	87.9 (1)	
		Isolated	6	–1.0	–1.0 (1)	1.7	1.7 (1)	95.4	95.4 (1)	
		Isolated	15	–23.4	–23.4 (1)	23.7	23.7 (1)	102.7	102.7 (1)	
		Isolated	9	–22.1	–22.1 (1)	23.4	23.4 (1)	94.4	94.4 (1)	
		Isolated	4	–24.0	–24.0 (1)	23.8	23.8 (1)	108.6	108.6 (1)	
		Isolated	8	–11.0	–11.0 (1)	15.0	15.0 (1)	110.8	110.8 (1)	
GC99-20 (Cable Head)	Calcite cement-2	Isolated	7	–17.1	–17.1 (1)	20.3	20.3 (1)	113.6	113.6 (1)	
		Cluster	7–12	–	–	–	–	108.9–112.5	107.8 (3)	
		Isolated	9	–	–	–	–	84.7	84.7 (1)	
		Isolated	10	–1.2	–1.2 (1)	2.1	2.1 (1)	107.2	107.2 (1)	
		Isolated	7	–0.6	–0.6 (1)	1.0	1.0 (1)	82.3	82.3 (1)	
	Calcite cement-2 (vein margin)	Cluster	6–8	–1.6	–1.6 (1)	2.7	2.7 (1)	90.7–101.2	96.0 (2)	
		Isolated	12	–0.6	–0.6 (1)	1.0	1.0 (1)	135.8	135.8 (1)	
		Isolated	7	–1.9	–1.9 (1)	3.2	3.2 (1)	130.1	130.1 (1)	
		Calcite cement-2 (vein center)	Cluster	4–7	–20.4– –22.0	–21.2 (2)	22.6–23.4	23.0 (2)	84.2–89.6	86.7 (4)
			Isolated	7	–20.4	–20.4 (1)	22.6	22.6 (1)	80.6	80.6 (1)

Table 2 (continued)

Sample no. (Formation)	Host mineral	Occurrence	Size (μm)	$T_{\text{m-ice}}(^{\circ}\text{C})$		Salinity (wt.% NaCl equiv.)		$T_{\text{h}}(^{\circ}\text{C})$	
				Range	Mean (n)	Range	Mean (n)	Range	Mean (n)
GC99-21 (Cable Head)	Calcite cement-2 (vein)	Isolated	12	–	–	–	–	115.5	115.5 (1)
		Isolated	3	–0.6	–0.6 (1)	1.0	1.0 (1)	118.8	118.8 (1)
		Isolated	4	–0.6	–0.6 (1)	1.0	1.0 (1)	113.9	113.9 (1)
		Cluster	5–9	–0.8	–0.8 (1)	1.4	1.4 (1)	92.8–95.4	94.1 (2)
		Isolated	6	–0.8	–0.8 (1)	1.4	1.4 (1)	97.2	97.2 (1)
GC-99-44 (Green Gables)	Calcite cement-2	Isolated	5	–	–	–	–	78.1	78.1 (1)
		Isolated	7	–23.6	–23.6 (1)	23.7	23.7 (1)	99.1	99.1 (1)
		Isolated	7	–24.9	–24.9 (1)	24.0	24.0 (1)	77.2	77.2 (1)
		Isolated	9	–25.4	–25.4 (1)	24.2	24.2 (1)	87.7	87.7
		Isolated	6	–	–	–	–	71.8	71.8 (1)
		Isolated	8	–1.7	–1.7 (1)	2.9	2.9 (1)	127.3	127.3 (1)
		Isolated	6	–1.2	–1.2 (1)	2.1	2.1 (1)	132.2	132.2 (1)
		Isolated	5	–1.4	–1.4 (1)	2.4	2.4 (1)	104.5	104.5 (1)
		Isolated	7	–1.1	–1.1 (1)	1.9	1.9 (1)	133.0	133.0 (1)
		GC99-47 (Green Gables)	Calcite cement-1	Isolated	8	–29.6	–29.6 (1)	25.4	25.4 (1)
Isolated	15			–23.0	–23.0 (1)	23.6	23.6 (1)	all liquid	all liquid
Calcite cement-2	Scattered		13–15	–24.3– –25.2	–24.8 (2)	24.3–24.7	24.5 (2)	106.2–122.4	114.3 (2)
	Isolated		10	–24.6	–24.6 (1)	24.0	24.0 (1)	116.7	116.7 (1)
	Isolated		4	–	–	–	–	110.3	110.3 (1)
	Isolated		8	–24.5	–24.5 (1)	23.9	23.9 (1)	144.6	144.6 (1)
	Isolated		6	–25.4	–25.4 (1)	24.2	24.2 (1)	88.4	88.4 (1)
	Isolated		9	–25.4	–25.4 (1)	24.2	24.2 (1)	125.9	125.9 (1)
	Isolated		7	–24.6	–24.6 (1)	24.0	24.0 (1)	93.9	93.9 (1)
	Isolated		10	–	–	–	–	104.8	104.8 (1)
GC99-65 (Bradelle)	Quartz cement	Isolated	8	–	–	–	–	111.2	111.2 (1)
		Isolated	5	–31.2	–31.2 (1)	26.0	26.0 (1)	75.4	75.4 (1)
		Isolated	4	–32.3	–32.3 (1)	26.3	26.3 (1)	67.3	67.3 (1)
		Isolated	9	–17.4	–17.4 (1)	20.5	20.5 (1)	80.5	80.5 (1)
		Isolated	7	–26.8	–26.8 (1)	24.6	24.6 (1)	71.1	71.1 (1)
GC99-75 (Bradelle)	Quartz cement	Isolated	7	–26.8	–26.8 (1)	24.6	24.6 (1)	71.1	71.1 (1)
		Isolated	8	–30.5	–30.5 (1)	25.7	25.7 (1)	all liquid	all liquid
		Isolated	6	–30.2	–30.2 (1)	25.6	25.6 (1)	all liquid	all liquid
	Calcite cement-2	Isolated	7	–	–	–	–	88.4	88.4 (1)
		Isolated	15	–36.9	–36.9 (1)	27.5	27.5 (1)	99.3	99.3 (1)
		Isolated	6	–	–	–	–	110.7	110.7 (1)
		Isolated	10	–33.9	–33.9 (1)	26.8	26.8 (1)	114.8	114.8 (1)
		Isolated	12	–	–	–	–	100.3	100.3 (1)
		Isolated	10	–29.4	–29.4 (1)	25.4	25.4 (1)	94.0	94.0 (1)
		Isolated	10	–	–	–	–	89.6	89.6 (1)
GC99-80 (Shepody)	Calcite cement-2	Isolated	10	–27.1	–27.1 (1)	24.6	24.6 (1)	86.1	86.1 (1)
		Isolated	4	–34.4	–34.4 (1)	26.9	26.9 (1)	122.7	122.7 (1)
		Isolated	5	–32.8	–32.8 (1)	26.5	26.5 (1)	133.3	133.3 (1)
		Isolated	3	–31.4	–31.4 (1)	26.0	26.0 (1)	129.1	129.1 (1)
		Cluster	8–9	–33.0	–33.0 (1)	26.5	26.5 (1)	95.4–102.7	100.1 (3)
		Isolated	12	–28.4	–28.4 (1)	25.1	25.1 (1)	134.6	134.6 (1)
		Isolated	11	–32.5	–32.5 (1)	26.4	26.4 (1)	120.9	120.9 (1)
		Isolated	11	–	–	–	–	108.2	108.2 (1)
		Isolated	8	–	–	–	–	105.8	105.8 (1)

Feldspar overgrowths are much less common than quartz overgrowths, and are mostly restricted to the Naufrage Formation (Table 1). Feldspar overgrowth is

CL non-luminescent, whereas the detrital feldspar shows blue luminescence. Both the detrital feldspar and its overgrowth were subject to later dissolution.

Most open pores are partly filled with very fine clay minerals, which appear to be the last diagenetic phases. In a few cases, green kaolinite clearly post-dates phase 2 calcite cement (Fig. 5N).

Using the above petrographic observations, the sequence of diagenetic minerals in the sandstones can be summarized as shown in Fig. 6. Precipitation of phase 1 calcite occurred early in the diagenesis. Some phase 1 calcite in calcareous clasts was formed before significant compaction. Quartz and feldspar cementation also started during early diagenesis, but quartz cementation may have also taken place in late diagenesis. With increasing burial, early calcite and feldspar cements as well as lithic grains were significantly dissolved, followed by widespread phase 2 calcite and quartz cementation events, which in turn were followed by a second phase of dissolution of calcite cement and framework grains. Finally, clay minerals were precipitated in residual pores. Although the above diagenetic sequence is generally applicable to every sample, a given diagenetic mineral phase in one sample is not always comparable to the same

mineral phase in another sample, because the whole stratigraphic column spans a time interval of more than 30 Ma. Thus, when the Naufrage Formation was being deposited, the Shepody Formation had already been subjected to significant burial diagenesis.

Petrographic observation suggests that the porosity of a sandstone sample is related to the amount of calcite cement such that when the amount of calcite cement is higher than 10%, the porosity is lower than 2.4% (mostly close to 0). On the other hand, when the amount of calcite cement is lower than 8.2% (mainly < 5%), the porosity may vary from 2% to 28% and is unrelated to the amount of calcite cement (Fig. 7A). There is a broad negative correlation between porosity and the amount of quartz cement: high percentage of quartz cement is related to low porosity, but low percentage of quartz cement may be related to either high or low porosity (Fig. 7B). The percentage of quartz cement generally increases with depth, although low percentages of quartz cement can be found throughout the entire drilled interval (Fig. 7C).

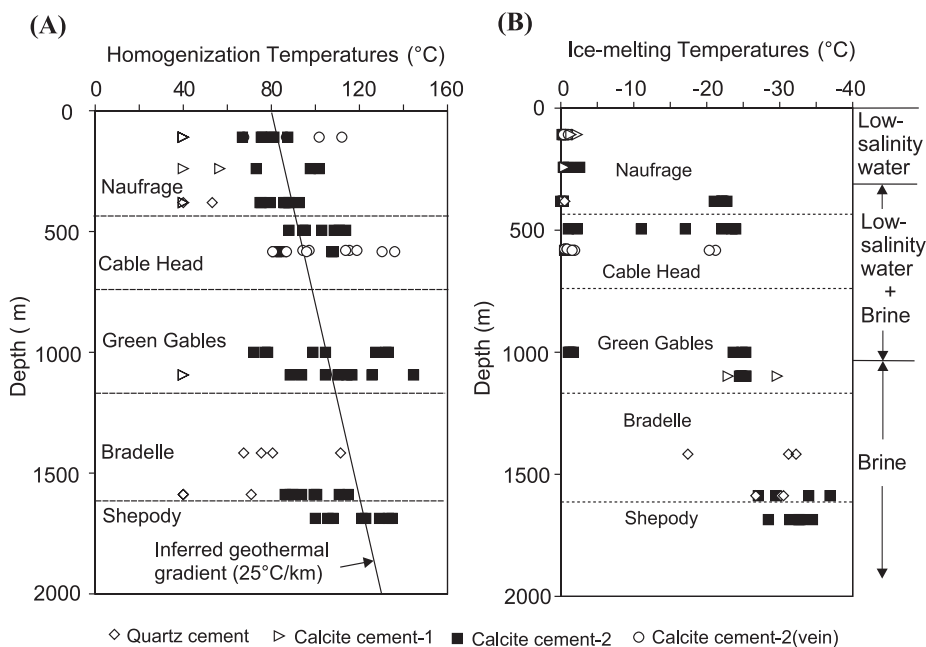


Fig. 8. (A) Distribution of fluid-inclusion homogenization temperatures of various diagenetic mineral phases with respect to drill depth. Also shown is an inferred geothermal gradient of 25 °C/km. (B) Distribution of fluid-inclusion ice-melting temperatures of various diagenetic mineral phases with respect to drill depth. The upper part was dominated by low-salinity water, the middle part by mixed low-salinity water and brine, and the lower part by brine.

5. Fluid inclusions

Eleven doubly polished thin sections were examined for fluid inclusions. Fluid inclusions that are isolated, clustered, or randomly distributed are considered primary or pseudosecondary inclusions. Workable fluid inclusions were generally difficult to find in quartz and feldspar cements, and most fluid inclusion data were obtained from calcite cements. The microthermometric data are presented in Table 2, and are illustrated with respect to depth in Fig. 8. Fluid inclusions in quartz and phase 1 calcite cements are typically monophasic (all liquid) at room temperature, suggesting relatively low temperatures of formation, although higher homogenization temperatures (up to 111 °C) were also locally recorded in quartz cements (Fig. 8A). Homogenization temperatures in phase 2 calcite cements are generally variable between 70 and 130 °C, and show a general increase with depth (Fig. 8A). Such a trend appears to be consistent with a geothermal gradient of about 25 °C/km (Fig. 8A). Fluid inclusions in phase 2 calcite in the veins show higher homogenization temperatures than those in matrix (Fig. 8A).

Ice-melting temperatures range from –0.3 to –36.9 °C for the whole sample set, corresponding to salinities of 0.5–27.5 wt.% NaCl equivalent. However, there is a clear variation pattern in ice-melting temperatures with depth (Fig. 8B). Above 242 m (sample GC99-9), ice-melting temperatures are higher than –2.6 °C (mainly higher than –1.0 °C), regardless of different calcite cement phases. From 380 (sample GC99-11) to 999 m (sample GC99-44), ice-melting temperatures vary from –0.3 to –25.4 °C, with phase 1 calcite and quartz cements located at the high ice-melting temperature end, and phase 2 calcite extending over the whole range (Fig. 8B). From 1096 m (sample GC99-47) and downwards, ice-melting temperatures range from –17.4 to –36.9 °C (Fig. 8B).

6. Carbon and oxygen isotopes

Carbon and oxygen isotopes were analyzed from 18 carbonate samples, including 4 from veins, 2 from calcareous clasts, 2 from calcite replacing fossil plants, and 10 from interstitial calcite cement (Table

3). It was impossible to separate phase 1 and phase 2 calcites in the interstitial cements. Because phase 2 calcite is volumetrically much more important than phase 1 calcite, the results are believed to mainly reflect the signature of phase 2 calcite in the interstitial

Table 3
Carbon and oxygen isotopes of carbonates

Sample no.	Formation	Minerals	$\delta^{18}\text{O}$ ‰ (PDB)	$\delta^{13}\text{C}$ ‰ (PDB)
GC99-2-1	Naufrage	Calcite vein	–7.9	–6.5
GC99-2-2	Naufrage	Interstitial calcite cement	–5.5	–5.7
GC99-8	Naufrage	Interstitial calcite cement	–7.5	–6.1
GC99-9-1	Naufrage	Interstitial calcite cement	–8.2	–6.9
GC99-9-2	Naufrage	Calcareous clasts	–4.5	–8.0
GC99-15	Naufrage	Interstitial calcite cement	–6.6	–6.8
GC99-20-1	Cable Head	Calcite vein	–9.5	–6.6
GC99-20-2	Cable Head	Interstitial calcite cement	–8.8	–6.9
GC99-21-1	Cable Head	Calcite vein	–10.7	–7.7
GC99-21-2	Cable Head	Interstitial calcite cement	–6.4	–7.4
GC99-28-1	Cable Head	Calcite vein	–10.7	–8.5
GC99-28-2	Cable Head	Calcareous clasts	–1.9	–7.5
GC99-31	Cable Head	Interstitial calcite cement	–5.9	–9.4
GC99-44	Green Gables	Interstitial calcite cement	–9.5	–11.6
GC99-53	Bradelle	Calcite replacing plants	–7.0	–14.1
GC99-71	Bradelle	Calcite replacing plants	–7.0	–14.4
GC99-78	Shepody	Interstitial calcite cement	–11.2	–13.4
GC99-80	Shepody	Interstitial calcite cement	–15.3	–7.3

cements. The results are listed in Table 3, and illustrated in Fig. 9.

Different carbonate phases fall in different domains in the $\delta^{13}\text{C}$ – $\delta^{18}\text{O}$ diagram (Fig. 9A), all being significantly depleted in ^{13}C with respect to Late Carboniferous marine calcite (Veizer et al., 1999). The calcareous clasts are characterized by relatively high $\delta^{18}\text{O}$ values (-4.5‰ and -1.9‰), with $\delta^{13}\text{C}$ values of -8.0‰ and -7.5‰ PDB. Two samples of calcite that replaced fossil plants are characterized by relatively low $\delta^{13}\text{C}$ values (-14.1‰ and -14.4‰), with $\delta^{18}\text{O}$ being -7.0‰ . The $\delta^{13}\text{C}$ and $\delta^{18}\text{O}$ values of interstitial calcite cements range from -13.4‰ to

-5.7‰ , and from -15.3‰ to -5.5‰ , respectively. The calcites from the veins fall in the same field as the interstitial calcite cements; however, within individual samples, vein calcite is commonly depleted in ^{18}O with respect to interstitial calcites (Table 3).

Considering interstitial calcite cements alone, there is a clear trend of decreasing $\delta^{13}\text{C}$ and $\delta^{18}\text{O}$ values with increasing depths (Fig. 9B and C). Thus, $\delta^{18}\text{O}$ values decrease from -5.5‰ at 107 m (sample GC99-2) to -11.2‰ at 1652 m (GC99-78) and then further to -15.3‰ at 1685 m (GC99-80) (Fig. 9B and Table 3). $\delta^{13}\text{C}$ values decrease from -6.5‰ at 107 m (sample GC99-2) to -13.4‰ at 1652 m

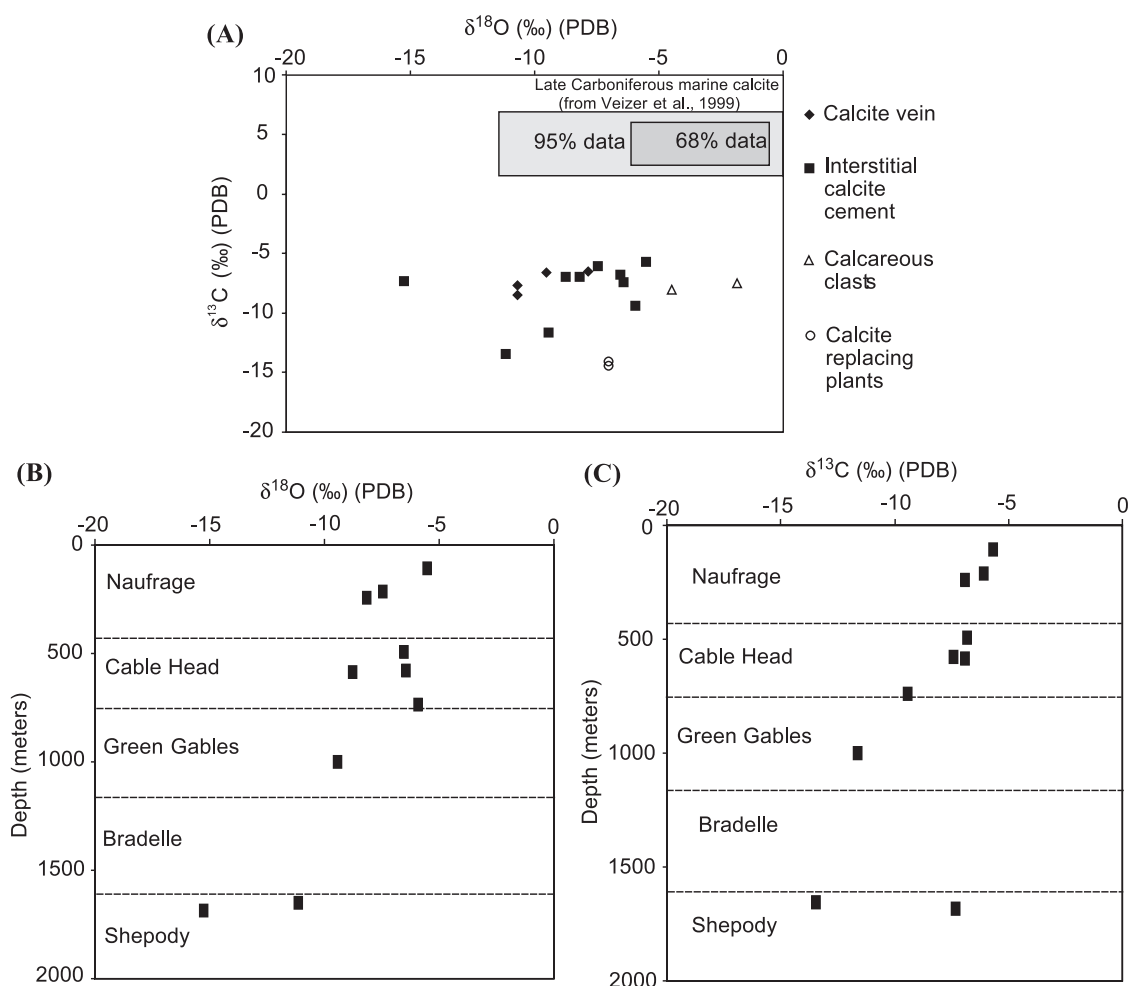


Fig. 9. (A) $\delta^{18}\text{O}$ – $\delta^{13}\text{C}$ diagram of various carbonate phases. (B) Distribution of $\delta^{18}\text{O}$ of interstitial calcite cements with respect to depth. (C) Distribution of $\delta^{13}\text{C}$ of interstitial calcite cements with respect to drill depth.

(GC99-78), and then back to -7.3% at 1685 m (GC99-80) (Fig. 9C and Table 3).

7. Organic matter petrography and maturity

Sixteen samples were treated for extraction of organic matter, and only seven yielded sufficient material for reflectance study. The initial objective was to evaluate the vertical variation of organic matter maturation in the entire drilled interval, but meaningful results were obtained only between 1210 and 1587 m. The results of the reflectance study are shown in Table 4.

Macerals, sub-macerals, and solid bitumens, recognized according to their host lithologies, are listed in Table 4. The maceral composition is clearly related to the lithology of the study sample. Inertinite (including fusinite, semifusinite and pseudovitrinite), mainly

semifusinite, dominate in sandstones. Vitrinite (including undifferentiated vitrinite, telinite, collotelinite, and gelinite) is found in four samples. Vitrinite composes the main part of organic matter in calcite replacing plants but it is also present in variable proportions in some sandstone samples. The plant tissue that is composed of telinite in calcite-replaced plant material is very well preserved. The tissue shows thin cellular walls and it is nearly uncompressed, suggesting that the replacement by calcite during the diagenesis was very early.

Vitrinite yields reflectance values from 0.53 to 0.63 (Table 4). Due to the short depth interval between these samples (from 1210 to 1587 m), it is not possible to see a variation pattern of vitrinite reflectance with depth. However, from these data it is clear that the strata were within the oil window.

Supramature solid bitumen, showing degassed, wavy anisotropy and mosaic structures (pyrobitumen),

Table 4
Results of petrography and reflectance analyses of organic matter

Sample no.	GC99-41	GC99-47	GC99-53	GC99-59	GC99-65	GC99-71	GC99-75
Lithology	Sandstone	Sandstone	Cal. rep. plant	Mudstone	Sandstone	Cal. rep. plant	Sandstone
Sporinite					0.18 ± 0.01 (2)		
Fusinite							1.83 ± 0.04 (18)
Semifusinite	1.61 ± 0.13 (50)		1.54 ± 0.06 (15)	1.41 ± 0.06 (4)	1.06 ± 0.26 (31)		1.17 ± 0.18 (22)
Pseudovitrinite		0.97 ± 0.05 (18)					
Undifferentiated vitrinite			0.57 ± 0.07 (22)		0.58 ± 0.04 (13)	0.57 ± 0.05 (9)	0.72 ± 0.02 (3)
Telinite			0.51 ± 0.07 (32)		0.62 ± 0.07 (11)	0.55 ± 0.06 (37)	0.55 ± 0.01 (3)
Collotelinite					0.69 ± 0.04 (14)		
Gelinite			0.43 ± 0.02 (9)			0.38 ± 0.03 (6)	
Protobitumen				1.19 ± 0.10 (9)			
Droplets of s. bitumen		0.41 ± 0.03 (12)	0.43 ± 0.01 (2)				
Isotropic solid bitumen				1.47 ± 0.29 (34)	0.61 ± 0.08 (6)		
Degassed s. bitumen				1.54 ± 0.02 (3)			
Wavy aniso. s. bitumen				1.50 ± 0.09 (21)			
Mosaic struct. s. bitumen				1.41 ± 0.07 (7)			
Graptolite-like bitumen				1.57 ± 0.02 (2)			
Average vitrinite ^a			0.53		0.63	0.55	0.63

Cal. rep. plant = Calcite replacing plant; s. bitumen = solid bitumen; aniso. = anisotropic; struct. = structure. 1.61 ± 0.13 (50) = mean reflectance % ± standard deviation (measurement number).

^a Weighted average of vitrinite, telinite, collotelinite, and gelinite.

makes up the major part of the organic content of mudstone. This pyrobitumen shows similar reflectance and petrography to that of pyrobitumen extracted from the Cambro-ordovician successions that composed the Humber Zone of Appalachian Belt (e.g., Bertrand, 1987). The measured reflectance of analyzed pyrobitumen indicates that the thermal maturity of the mudstone should be much higher than suggested by the vitrinite in sandstones and in calcite replacing plants (Bertrand, 1993), suggesting that the organic matter in the mudstone is likely recycled from older rocks.

8. Discussion

The purpose of this study was to characterize the porosity patterns and to evaluate their controlling factors in the Upper Carboniferous sandstones of the Spring Valley #1 well, thus providing a reference for understanding the diagenetic history and porosity evolution of equivalent sandstones in other parts of the Maritimes Basin. Our petrographic, fluid-inclusion, and carbon and oxygen isotopic results have shown regular changes in certain diagenetic features with depths. Based on these data, we will discuss the controlling factors on porosity evolution in this section. Among the most important factors are compaction, calcite and quartz cementation, and calcite and framework grain dissolution.

8.1. The role of compaction

The trend of decreasing porosity values with depth (Fig. 4) suggests that compaction of sediments played a major role in reducing porosities. Such a trend is also commonly found in other wells in the Maritimes Basin, although significant variation exists for specific depth levels (Bibby and Shimeld, 2000). In order to evaluate the role of compaction, it is useful to compare the porosity-depth data with a theoretical curve predicting sandstone porosity change with depth due to compaction. To construct the porosity–depth curve, it is necessary to know the burial history of the strata, especially maximum burial. For the Spring Valley #1 well, most strata have undergone a single burial–uplift (erosion) cycle, except for the Shepody Formation which was once buried, exposed (unconformity),

buried again, and then uplifted. It is therefore critical to know how much of the strata have been eroded. Based on apatite fission track studies, Ryan and Zentilli (1993) inferred that an additional 1.5–4 km of strata were deposited and subsequently eroded in the Maritimes Basin, assuming a paleogeothermal gradient of approximately 25 °C/km. It is difficult to estimate the maximum burial depth without a systematic burial analysis specific to the Spring Valley #1 well. However, several lines of evidence suggest that the uppermost strata in the Spring Valley #1 well were probably subjected to a maximum burial depth of 1–2.5 km. The fluid inclusion homogenization temperatures of phase 2 calcite cements are consistent with a paleogeothermal gradient of 25 °C/km (Fig. 8A). If the maximum burial temperature of the top-most of the section is taken as 80 °C, and a paleo-surface temperature of 20 °C is assumed, the thickness of eroded strata is estimated to be 2.4 km. The vitrinite reflectance values are 0.53 (1210 m), 0.63 (1418 m), 0.57 (1489 m) and 0.63 (1586 m). These vitrinite reflectance values correspond to temperatures of 77, 99, 86, and 99 °C, respectively, according to Barker and Goldstein's (1990) equation. Using a paleo-surface temperature of 20 °C and a paleogeothermal gradient of 25 °C/km, these temperatures correspond to maximum burial depths of 2.3, 3.2, 2.6, and 3.2 km, respectively. This indicates erosion of 1.1–1.8 km of strata. Thus, the total erosion thickness inferred from the fluid inclusion and vitrinite reflectance data ranges from 1.1 to 2.4 km. In the following discussion, an average erosion thickness of 1.75 km is used.

A comparison of the porosity–depth data with the “normal” compaction curve of sandstones (Bethke, 1985), based on the assumption of 1.75 km of additional strata, shows three different clusters of porosity data (Fig. 10). Group “A” shows near-zero porosity regardless of the depth. Group “B”, mainly from the upper part of the Bradelle Formation to the lower part of the Naufrage Formation, shows porosity values higher than the compaction curve (Fig. 10). Group “C”, mainly in the Bradelle and Shepody formations, has porosity values lower than the compaction curve (Fig. 10). Although the compaction curve specific to the sandstones of this study is not known, and is possibly deviated from the one shown on Fig. 10, it is likely that the porosities in Group

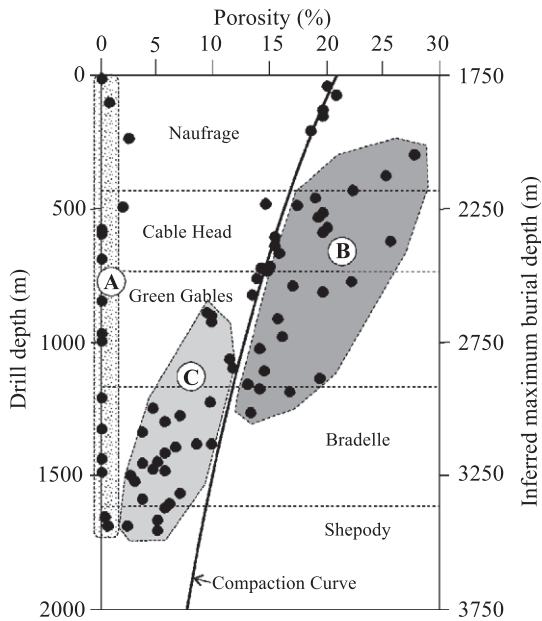


Fig. 10. Comparison between measured sandstone porosity data with the theoretical compaction curve predicted for sandstones. The compaction curve was constructed with Bethke's (1985) equation, with the assumption of an additional 1.75 km burden before erosion. The meanings of fields A, B, and C are discussed in the text.

“B” have been enhanced relative to the compaction porosities.

Group “A” is characterized by very high percentages of calcite cement (see Figs. 5E and 7A), which was formed in the early stage of diagenesis (phase 1 calcite) and was largely transformed to phase 2 calcite in the late stage of diagenesis. It appears that abundant early calcite cementation, which almost completely occluded the primary porosities, is unfavorable for porosity preservation and later development of secondary porosity. Group “C” was subject to significant compaction, and although the observed dissolution of calcite cement and framework grains generated secondary porosity, much of it and residual primary porosity were filled by later quartz and calcite cements. The net porosity is thus lower than expected from normal compaction. Two factors could have contributed to the development of higher-than-normal porosities in Group “B”. One is early (but minor) cementation (quartz, feldspar, and calcite) in primary pore space which increased the framework strength of the sediments and preserving primary

porosity from compaction reduction. The other factor is the dissolution of the early calcite cement and metastable framework grains (feldspars and lithic grains) which created secondary pores and/or enlarged the preserved primary pores (Fig. 5A and B). Although various cements were also present in this group, the net increase of porosity through dissolution was higher than the reduction through cementation, resulting in porosities higher than expected from normal compaction.

8.2. Calcite cementation

Calcite cementation played a key role in the porosity evolution of the sandstones. Petrographic evidence indicates that calcite cements were formed early in diagenesis, which were subjected to dissolution, and followed by precipitation of new calcite cements in later diagenesis. The early calcite cementation played a constructive role in porosity preservation because it could prevent significant early mechanical compaction and its dissolution in later diagenesis could generate secondary porosity. However, where early cementation was abundant and almost completely occluded primary porosity, later dissolution was compensated by re-precipitation of calcite and no new porosity was created. In contrast, where early calcite cementation was minor but sufficient to strengthen the framework against compaction, its role for porosity preservation is optimized. New porosity was generated if the dissolution of this early calcite cement was not compensated by new cement formation, which appears to be the case for Group “B” in Fig. 10.

Fluid inclusions in early calcite cements are mono-phase (all liquid) (Table 2 and Fig. 8A), indicating low temperatures of formation. In the upper part of stratigraphic column, the ice-melting temperatures are generally higher than -1.0 °C, indicating lower-than-seawater salinities, whereas in the lower part of the stratigraphic section, saline fluids were present during early calcite and quartz cementation (Table 2 and Fig. 8B). Carbon and oxygen isotopes of the early calcite cements were not obtained because they are mixed with and volumetrically much less important than later calcite cements. However, two samples of calcareous clasts, which share CL features with the early calcite cements, were successfully separated for carbon and oxygen isotope analysis. These two cal-

careous clasts are characterized by low $\delta^{13}\text{C}$ values (-7.5‰ and -8.0‰ PDB), similar to later calcite cement, and by relatively high $\delta^{18}\text{O}$ values (-1.9‰ and -4.5‰ PDB) with respect to later calcite cements (Table 3 and Fig. 9A). Although the $\delta^{18}\text{O}$ values fall well within the range of Carboniferous marine calcite (Fig. 9A; Veizer et al., 1999), they do not necessarily indicate pristine marine values. In fact, the sandstones were deposited in a continental environment, and the interstitial pore water must have been of meteoric origin. Furthermore, the two calcareous clast samples are from the upper part of the stratigraphic column (above 694 m), where fluid-inclusion data indicate lower-than-seawater salinities for early calcite cements. Paleomagnetic studies have shown that the Maritimes Basin was located near the equator in late Carboniferous (Scotese et al., 1984). This suggests that the oxygen isotope composition of meteoric water was probably close to that of seawater. The carbon isotope results suggest that a significant part of the carbon of the calcareous clasts, and by inference that of early calcite cements, was derived from organic matter.

Phase 2 calcite cementation likely took place under significant burial. The fact that phase 2 calcite also occurs in fractures indicates that this phase of calcite cementation took place after a phase of fracturation. Homogenization temperatures of fluid inclusions range mainly from 70 to 130 °C, and show an overall increase with depth (Fig. 8A). Ice-melting temperatures of fluid inclusions indicate lower-than-seawater salinity in the upper part, mixed low-salinity waters and brines in the middle, and brines in the lower part (Fig. 8B). Brines with similar salinities have been recorded by fluid inclusions in Mississippi Valley-type ore deposits in the basal part of the Windsor Group (Chi et al., 1998), and as formation waters in Upper Carboniferous sandstones in the Sydney coal-field (Martel et al., 2001). The low-salinity waters could have been connate or recharged meteoric waters, whereas the brines were most likely derived from the underlying evaporites in the Windsor Group. Brine circulation was probably driven by overpressures developed within the Windsor Group (Chi and Savard, 1998). However, the upward movement of the brine was probably slow, because the homogenization temperatures of the brine inclusions are not abnormally high (Fig. 8). The $\delta^{18}\text{O}$ values of late pore-filling

calcite cements show a decreasing trend with depth (Fig. 9B), which agrees with normal temperature increase with depth. The $\delta^{13}\text{C}$ values of late calcite cements (-13.4‰ to -5.7‰) also decrease with depth (Fig. 9C). As for early calcite cements, the low $\delta^{13}\text{C}$ values suggest that a significant portion of the bicarbonate ions were derived from organic sources. The decrease in $\delta^{13}\text{C}$ with depth indicates either increasing proportion of organic carbon or decreasing $\delta^{13}\text{C}$ values of the organic carbon. It is inferred that more and more CH_4 , characterized by very low $\delta^{13}\text{C}$ values, was generated with increasing burial, the oxidation of which provided ^{13}C -depleted carbon for calcite precipitation.

8.3. Formation of secondary porosities

Petrographic studies have shown extensive dissolution of calcite cement and framework grains, especially feldspar. A number of processes have been proposed in the literature to explain the dissolution of calcite and feldspar in sandstones. Among these the most important are (1) reactions with meteoric waters; (2) reactions with CO_2 derived from organic matter maturation; (3) reactions with organic acids; and (4) inorganic mineral reactions.

Pristine meteoric waters are undersaturated with carbonates and feldspars, and H^+ produced through decomposition of vegetation is largely responsible for their leaching capacity (Bjorlykke, 1984). Wang (1992) related secondary porosity generation in Carboniferous sandstones of Northern Ireland to dissolution of carbonate cements by meteoric water, accompanied by reddening of the sandstones. Our fluid-inclusion data indicate that interstitial fluids in the upper part of the Spring Valley #1 well (the Naufrage Formation) were dominated by fluids with lower-than-seawater salinities in the entire diagenetic history (Fig. 8B). Pore space in the middle part of the stratigraphic column (the Cable Head Formation and the upper part of the Green Gables Formation) was also filled by these low-salinity fluids, although it was later invaded by brines. It has also been observed that the upper and middle parts of the stratigraphic column are dominated by relatively porous red-colored sandstones (Table 1 and Fig. 4). Based on these observations, we infer that the dissolution of calcite cements and framework grains was at least partly related to the

incursion of meteoric waters, especially in the early stage of diagenesis.

CO₂ released from organic matter maturation has been generally considered a potential agent for carbonate and feldspar dissolution (Schmidt and McDonald, 1979), although the amount of CO₂ may not be sufficient to explain the amount of secondary porosities produced by carbonate and feldspar dissolution (e.g., Bjorlykke, 1984; Land, 1984). On the other hand, Surdam et al. (1984) proposed that carboxylic acids derived from organic matter maturation were efficient agents for dissolution of both carbonates and aluminosilicates, with aluminum-organic complexes being removed from the local diagenetic system. The oxidation of organic matter could generate both CO₂ and organic acids (e.g., Shebl and Surdam, 1996). Considering the possible infiltration of meteoric waters, the oxidizing capacity of the red-colored sandstones, and the possible high SO₄²⁻ concentrations in the brines derived from the underlying Windsor evaporites, it is likely that significant amounts of CO₂ and organic acids were generated in the Upper Carboniferous sandstones.

According to Surdam et al. (1984), the concentration of carboxylic acids increases with burial temperatures, peaks at around 80 °C, and then decreases with increasing temperatures. Thus, they proposed that, in a diagenetic realm with significant carboxylic acids, calcite precipitation should dominate at shallow (<70 °C) and deep (>140 °C) burial, whereas calcite dissolution is expected at moderate burial (70–140 °C). Although not in exact agreement in terms of temperature range, our fluid-inclusion, stable isotope, and porosity data generally agree with such a model.

9. Conclusions and implications for reservoir development

This study shows that significant porosities have been developed in the Upper Carboniferous sandstones of the Maritimes Basin, which may form good hydrocarbon reservoirs if coupled with favorable source and trapping conditions. Favorable conditions for porosity development include: (1) shallow burial (preservation of significant primary porosity), (2) early calcite cementation which was sufficient to strengthen the framework against physical compac-

tion but did not completely occlude primary porosity, and (3) significant dissolution of calcite cements and framework grains which generated significant secondary porosity.

The upper and middle parts of the stratigraphic column from the Spring Valley #1 well (the Naufrage, Cable Head, and Green Gables formations) show porosity values higher than those that could have been expected from normal mechanical compaction. This high-porosity interval coincides with significant reddening of the sandstones and a fresh water-dominated regime as indicated by fluid-inclusion data, implying that reaction with meteoric water may have played a major role in secondary porosity development. This interval also broadly corresponds to the hypothetical peak of carboxylic acids concentrations. As suggested by the low δ¹³C values of carbonate cements, organic matter may have played an important role in the diagenetic evolution of the sandstones. The CO₂ and organic acids generated from maturation and oxidation of organic matter, in addition to meteoric waters, were likely responsible for calcite and feldspar dissolution.

Similar diagenetic processes could have taken place in the Upper Carboniferous sandstones in other parts of the Maritimes Basin. Thus, despite the Paleozoic age of the basin, which is generally considered less favorable for reservoir development in comparison with younger (Mesozoic and Cenozoic) basins, significant porosities could be developed and preserved, especially in the upper part of the sedimentary succession. However, a regional-scale, three-dimensional pattern of reservoir development, which could be used in hydrocarbon exploration, requires more extensive and integrated basin analysis and diagenetic studies.

Acknowledgements

This paper is a Geological Survey of Canada Contribution (2000251). The study was part of a project dealing with the hydrocarbon systems of the western Maritimes Basin, financially supported by Program of Energy Research and Development (PERD) of the Energy Sector of Natural Resources Canada. We would like to thank Charmain Bibby and John Shimeld, GSC-Atlantic, for assistance in literature search, and the staff in the Stellarton Core

Library, Nova Scotia Department of Natural Resources, for their assistance in core sampling. Dr. N. Tassé of INRS-Eau, Terre et Environnement is thanked for reviewing the manuscript. The constructive comments by two JGE reviewers, and by Editor-in-Chief Dr. Rudy Swennen have helped improve the quality of the paper.

References

- Barker, C.E., Goldstein, R.H., 1990. Fluid-inclusion technique for determining maximum temperature in calcite and its comparison to vitrinite reflectance geothermometer. *Geology* 18, 1003–1006.
- Bertrand, R., 1987. Maturation thermique et potentiel pétrolière des séries post-taconiennes du nord-est de la Gaspésie et de l'île d'Anticosti. Doctorate thesis, University of Neuchâtel, Switzerland. 647 pp.
- Bertrand, R., 1993. Standardization of solid bitumen reflectance to vitrinite in some Paleozoic sequences of Canada. *Energy Sources Journal* 15, 269–288.
- Bertrand, R., Héroux, Y., 1987. Chitinozoan, graptolite and scolecodont reflectance as an alternative to vitrinite and pyrobitumen reflectance in Ordovician and Silurian strata, Anticosti Island, Québec, Canada. *AAPG Bulletin* 71, 951–957.
- Bertrand, R., Bérubé, J.-C., Héroux, Y., Achab, A., 1985. Pétrographie du kérogène dans le Paléozoïque inférieur: méthode de préparation et exemple d'application. *Revue de l'Institut français du Pétrole* 40, 155–167.
- Bethke, C.M., 1985. A numerical model of compaction-driven groundwater flow and heat transfer and its application to the paleohydrology of intracratonic sedimentary basins. *Journal of Geophysical Research* 90, 6817–6828.
- Bibby, C., Shimeld, J., 2000. Compilation of reservoir data for sandstones of the Devonian-Permian Maritimes Basin, eastern Canada. Geological Survey of Canada, Open File 3895.
- Bjorlykke, K., 1984. Formation of secondary porosity: how important is it? In: McDonald, D.A., Surdam, R.C. (Eds.), *Clastic Diagenesis*. AAPG Memoir, vol. 37, pp. 277–286.
- Blatt, H., 1992. *Sedimentary petrology*, 2nd ed. W.H. Freeman and Company, New York. 514 pp.
- Chi, G., Savard, M.M., 1998. Basinal fluid flow models related to Pb–Zn mineralization, southern margin of the Maritimes Basin. *Economic Geology* 93, 896–910.
- Chi, G., Savard, M.M., 1999. Oil inclusions in the Jubilee Zn–Pb deposit, Nova Scotia – Evidence of an exhausted oil reservoir. *Hydrocarbon-Bearing Inclusions in Crustal Rocks— Study Methods, Applications and Case Histories*, Mineralogical Society of Great Britain and Ireland Spring Meeting, Galway, Ireland, April 7–8, 1999. 1 p.
- Chi, G., Kontak, D.J., Williams-Jones, A.E., 1998. Fluid composition and thermal regime during base-metal mineralization in the lower Windsor Group, Nova Scotia. *Economic Geology* 93, 911–919.
- Chowdhury, A.H., Noble, J.P.A., 1992. Porosity evolution in the Albert Formation of the Stoney Creek oil and gas field, Moncton Subbasin, New Brunswick, Canada. *AAPG Bulletin* 76, 1325–1343.
- Chowdhury, A.H., Fowler, M.G., Noble, J.P.A., 1991. Petroleum geochemistry and geology of the Alberta Formation, Moncton Subbasin, New Brunswick, Canada. *Bulletin of Canadian Petroleum Geology* 39, 315–331.
- Dickson, J.A.D., 1965. A modified staining technique for carbonates in thin section. *Nature* 205, 587.
- Fowler, M.G., Hamblin, A.P., MacDonald, D.J., McMahon, P.G., 1993. Geological occurrences and geochemistry of some oil shows in Nova Scotia. *Bulletin of Canadian Petroleum Geology* 41, 422–436.
- Gibling, M.R., Nguyen, M.H., 1999. Diagenetic and burial history of Sydney Basin sandstones. In: Gibling, M.R., Martel, A.T., Nguyen, M.H. (Eds.), *Geology and Hydrogeology of the Subsea Mining District, Sydney Coalfield, Nova Scotia*. Centre for Marine Geology, Dalhousie University. Technical Report 14, 3-1 to 3-74.
- Giles, P.S., Utting, J., 1999. Maritimes Basin stratigraphy-Prince Edward Island and adjacent Gulf of St. Lawrence. Geological Survey of Canada. Open File 3732.
- Hamblin, A.P., Fowler, M.G., Utting, J., Hawkins, D., Riediger, C.L., 1995. Sedimentary, palynology and source rock potential of Lower Carboniferous (Tournaesian) rocks, Conche Area, Great Northern Peninsula, Newfoundland. *Bulletin of Canadian Petroleum Geology* 43, 1–19.
- Kalkreuth, W., Macauley, G., 1987. Organic petrology and geochemical (Rock-Eval) studies on oil shales and coals from the Pictou and Antigonish areas, Nova Scotia, Canada. *Bulletin of Canadian Petroleum Geology* 35, 263–295.
- Land, L.S., 1984. Frio sandstone diagenesis, Texas Gulf Coast: a regional isotopic study. In: McDonald, D.A., Surdam, R.C. (Eds.), *Clastic Diagenesis*. AAPG Memoir, vol. 37, pp. 47–62.
- Lavoie, D., Sami, T., 1998. Sedimentology of the lowest Windsor carbonate rocks: base metal hosts in the Maritimes Basin of eastern Canada. *Economic Geology* 93, 719–733.
- Martel, A.T., Gibling, M.R., Nguyen, M., 2001. Brines in the Carboniferous Sydney coalfield, Atlantic Canada. *Applied Geochemistry* 16, 35–55.
- Pittman, E.D., 1992. Artifact porosity in thin sections of sandstones. *Journal of Sedimentary Petrology* 62, 734–737.
- Ryan, R.J., Zentilli, M., 1993. Allocyclic and thermochronological constraints on the evolution of the Maritimes Basin of eastern Canada. *Atlantic Geology* 29, 187–198.
- Ryan, R.J., Boehner, R.C., Calder, J.H., 1991. Lithostratigraphic revisions of the upper Carboniferous to lower Permian strata in the Cumberland Basin, Nova Scotia and the regional implications for the Maritimes Basin in Atlantic Canada. *Bulletin of Canadian Petroleum Geology* 39, 289–314.
- Schmidt, V., McDonald, D.A., 1979. Textures and recognition of secondary porosity in sandstones. In: Scholle, P.A., Schluger, P.R. (Eds.), *Aspects of Diagenesis*, vol. 26. SEPM Special Publication, pp. 209–225.
- Scotese, C.R., Van der Voo, R., Johnson, R.E., Giles, P.S., 1984. Paleomagnetic results from the Carboniferous of Nova Scotia.

- In: Van der Voo, R., Scotese, C.R., Bonhommet, N. (Eds.), Plate Reconstruction from Paleozoic Paleomagnetism. American Geophysical Union, Geodynamics Series, vol. 12, pp. 63–81.
- Shebl, M.A., Surdam, R.C., 1996. Redox reactions in hydrocarbon clastic reservoirs: experimental validation of this mechanism for porosity enhancement. *Chemical Geology* 132, 103–117.
- St. Peter, C., 1993. Maritimes Basin evolution: key geologic and seismic evidence from the Moncton Subbasin of New Brunswick. *Atlantic Geology* 29, 233–269.
- Surdam, R.C., Boese, S.W., Crossey, L.J., 1984. The chemistry of secondary porosity. In: McDonald, D.A., Surdam, R.C. (Eds.), *Clastic Diagenesis*. AAPG Memoir, vol. 37, pp. 127–149.
- Taylor, G.H., Teichmüller, M., Davis, A., Diessel, C.F.K., Littke, R., Robert, P., 1998. *Organic Petrology*. Gebrüder Borntraeger, Berlin-Stuttgart. 704 pp.
- van de Poll, H.W., Gibling, M.R., Hyde, R.S., 1995. Upper Paleozoic rocks. In: Williams, H. (Ed.), Chapter 5 of *Geology of the Appalachian–Caledonian Orogen in Canada and Greenland*; Geological Survey of Canada. *Geology of Canada*, vol. 6, pp. 449–566.
- Veizer, J., Ala, D., Azmy, K., Bruckschen, P., Buhl, D., Bruhn, F., Carden, G.A.F., Diener, A., Ebner, S., Godderis, Y., Jasper, T., Korte, C., Pawellek, F., Podlaha, O.G., Strauss, H., 1999. $^{87}\text{Sr}/^{86}\text{Sr}$, $\delta^{13}\text{C}$ and $\delta^{18}\text{O}$ evolution of Phanerozoic seawater. *Chemical Geology* 161, 59–88.
- Wang, W.H., 1992. Origin of reddening and secondary porosity in Carboniferous sandstones, Northern Ireland. In: Parnell, J. (Ed.), *Basins on the Atlantic Seaboard: Petroleum Geology, Sedimentology and Basin Evolution*, vol. 62. Geological Society Special Publication, pp. 243–254.
- Williams, E.P., 1974. Geology and petroleum possibilities in and around Gulf of St. Lawrence. *AAPG Bulletin* 58, 1137–1155.